

Dynamics of flow pattern in baffled mixing vessel with axial impeller

O. Brůha,^a T. Brůha,^b I. Fořt,^c M. Jahoda^b

^a*Department of Physics, Faculty of Mechanical Engineering, Czech Technical University, Technická 4, CZ - 166 07 Praha 6, Czech Republic*

^b*Department of Chemical Engineering, Institute of Chemical Technology, Prague, Technická 5, CZ - 166 28 Praha 6, Czech Republic*

^c*Department of Process Engineering, Faculty of Mechanical Engineering Czech Technical University, Technická 4, CZ - 166 07 Praha 6, Czech Republic*

Abstract

This paper deals with the primary circulation of an agitated liquid in a flat-bottomed cylindrical stirred tank. The study is based on experiments, and the results of the experiments are followed by a theoretical evaluation. The vessel was equipped with four radial baffles and stirred with a six pitched blade impeller pumping downwards. The experiments were concentrated on the lower part of the vessel, the origin of space pulsations of the primary loop, initiated by the pumping of the impeller action. This area is considered to be the birthplace of the flow macroinstabilities in the system - a phenomenon which has been studied and described by several authors. The flow was observed in a vertical plane passing through the vessel axis. The flow patterns of the agitated liquid were visualized by means of *Al* micro particles illuminated by a vertical light knife and scanned by a digital camera. The experimental conditions corresponded to the turbulent regime of agitated liquid flow.

It was found that the primary circulation loop is elliptical in shape. The main diameter of the primary loop is not constant. It increases in time and after reaching a certain value the loop disintegrates and collapses. This process is characterized by a certain periodicity and its period proved to be correlated to the occurrence of flow macroinstability. The instability of the loop can be explained by a dissipated energy balance. When the primary loop reaches the level of disintegration, the whole impeller power output is dissipated and under this condition any flow alteration requiring additional energy, even a very small vortex separation, causes the loop to collapse.

Keywords: mixing, axial impeller, primary circulation loop, oscillation, macroinstability

1. Introduction

A mechanically agitated system under a turbulent regime of flow with or without internals (radial baffles, draft tubes, coils etc.) consists of a broad spectrum of eddies from the size of the main (primary) circulation loop (PCL) of the agitated batch down to the dissipative vortices corresponding to micro-scale eddies.

This study deals with experimental and theoretical analysis of the behaviour of the flow pattern, and mainly the PCL in an agitated liquid in a system with an axial flow impeller and radial baffles. Some characteristics of the investigated behaviour are considered to be in correlation with the occurrence of flow macroinstabilities (FMIs), i.e. the flow macro-formation (vortex) appearing periodically in various parts of a stirred liquid. The flow macroinstabilities in a mechanically agitated system are large-scale variations of the mean flow which may affect the structural integrity of the vessel internals and can strongly affect both the mixing process and the measurement of turbulence in a stirred vessel. Their space and especially time scales considerably exceed those of the turbulent eddies, that are a well known feature of mixing systems. The FMIs occurs in a range from several up to tens of seconds in dependence on the scale of the agitated system. This low-frequency phenomenon is therefore quite different from the main frequency of an incompressible agitated liquid corresponding to the frequency of revolution of the impeller.

Generally, experimental detection of FMIs is based on frequency analysis of the oscillating signal (velocity, pressure, force) in long time series and frequency spectra, or more sophisticated procedures (proper orthogonal decomposition of the oscillating signal, the Lomb period gram or the velocity decomposition technique) are used to determine the FMI frequencies. Theoretical finding of FMIs could contribute significantly to a deeper understanding of fluid flow behaviour in stirred vessels, e.g. a description of the circulation patterns of a agitated liquid, application of the theory of deterministic chaos, knowledge of turbulent coherent structures, etc. [1-10].

This study investigates oscillations of the primary circulation loop (the source of FMIs) in a cylindrical system with an axial flow impeller and radial baffles, aiming at a theoretical description of the hydrodynamical stability of the loop. However, no integrated theoretical study of the MI phenomenon has been presented up to now.

2. Experimental

The experiments were performed in a flat-bottomed cylindrical stirred tank of inner diameter $T = 0.29$ m filled with water at room temperature with the tank diameter height $H = T$. The vessel was equipped with four radial baffles (width of baffles

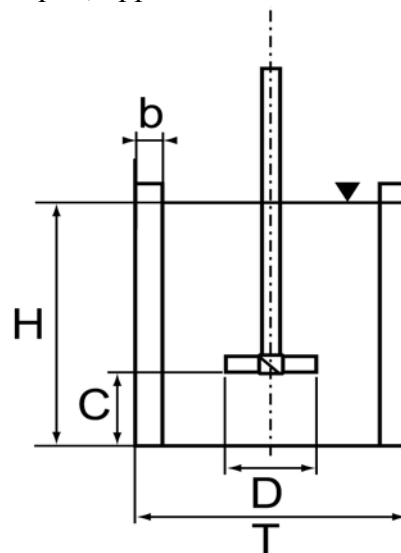


Fig. 1. Pilot plant experimental equipment.

$b = 0.1T$) and stirred with six pitched blade impeller (pitch angle 45° , diameter $D = T/3$, width of blade $W = D/5$), pumping downwards. The impeller speed was adjusted $n = 400 \text{ rpm} = 6.67 \text{ s}^{-1}$ and its off-bottom clearance C was $T/3$ (see Fig. 1).

The flow under the parameters mentioned above was turbulent, with the impeller Reynolds number value $Re_M = 6.22 \cdot 10^4$.

The flow was observed in a vertical plane passing through the vessel (vertical section of the vessel) in front of the adjacent baffles. The flow patterns of the agitated liquid were visualized by means of Al micro particles 0.05 mm in diameter spread in water and illuminated by a vertical light knife 5 mm in width, see Fig. 2.

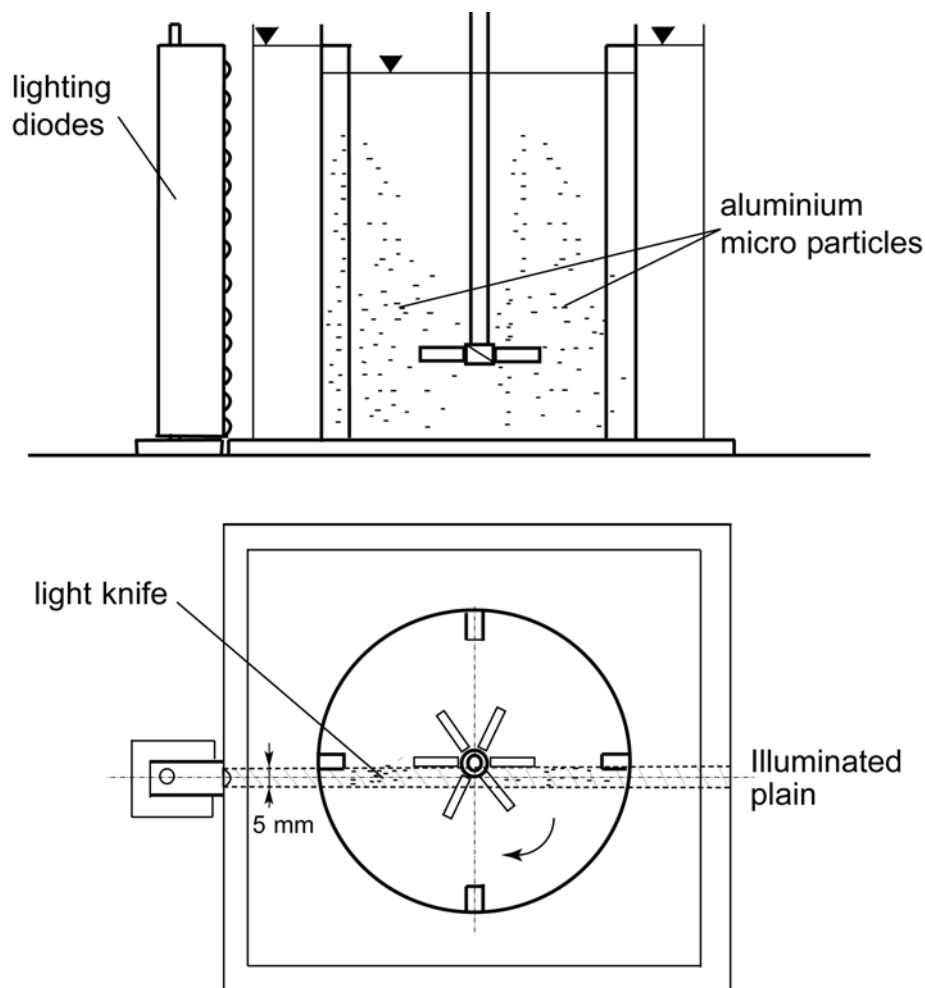


Fig. 2. Experimental technique of flow visualization.

The visualized flow was scanned by a digital camera; series of shots were generated with a time step of 0.16 s and were analyzed by appropriate graphic software. The total length of the analyzed record was 30.24 s. The characteristics observed and analyzed were:

- a) the shape and sizes of the PCL,
 - b) the size of the PCL core,
 - c) the positions of the top of the flow macro formation
- and the corresponding functions were obtained:

- a) the height of the PCL $h_{ci} = h_{ci}(t)$ (see Fig. 3),
- b) the width of the PCL $s_{ci} = s_{ci}(t)$ (see Fig. 3),
- c) the equivalent mean diameter of the PCL core $r_{c,av i} = r_{c,av i}(t)$ (see Fig. 3),
- d) the height of the top of the flow macro formation $h_{FMI,i} = h_{FMI,i}(t)$ (see Fig. 4).

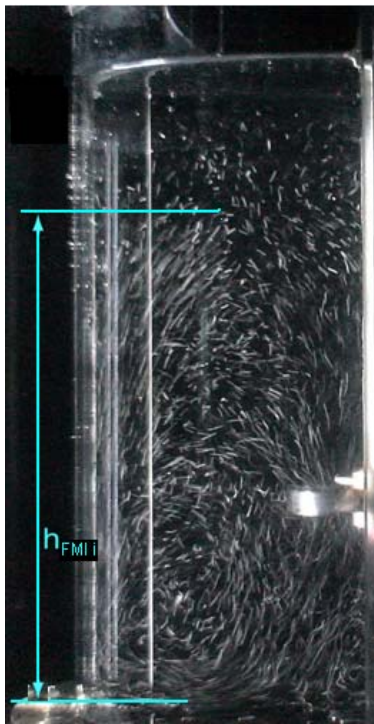


Fig. 3. Visualization of the PCL.

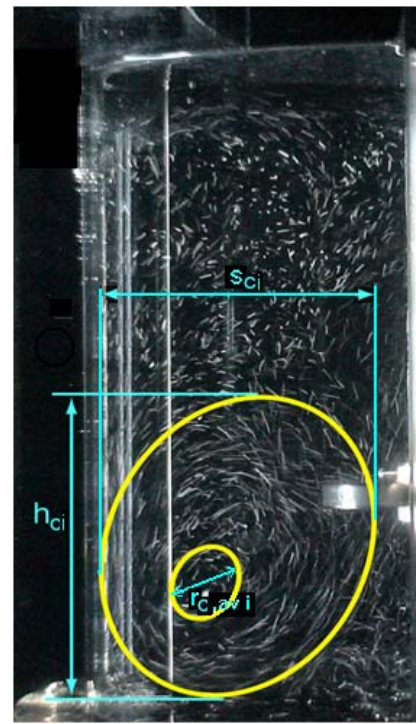


Fig. 4. Visualization of flow macro formation.

3. Results of experiments

The analysis of the experiments provided the following findings:

The PCL can be described as a closed stream tube with a vertical section elliptical in shape with a core. The flow in the elliptical annular area is intensive and streamlined, while the core is chaotic and has no apparent streamline characteristics. The flow in the remaining upper part is markedly steadier. This is in agreement with the earlier observations of some authors [6, 7].

The flow process is characterized by three stages. In the first stage, the PCL grows to a certain size (its shape can be approximated as elliptical). Then a quasi-steady stage follows, when the PCL remains at a constant size for a short time. In the next stage

the PCL collapses into very small flow formations (vortices) or disintegrates into chaotic flow, see Fig. 5a-c.

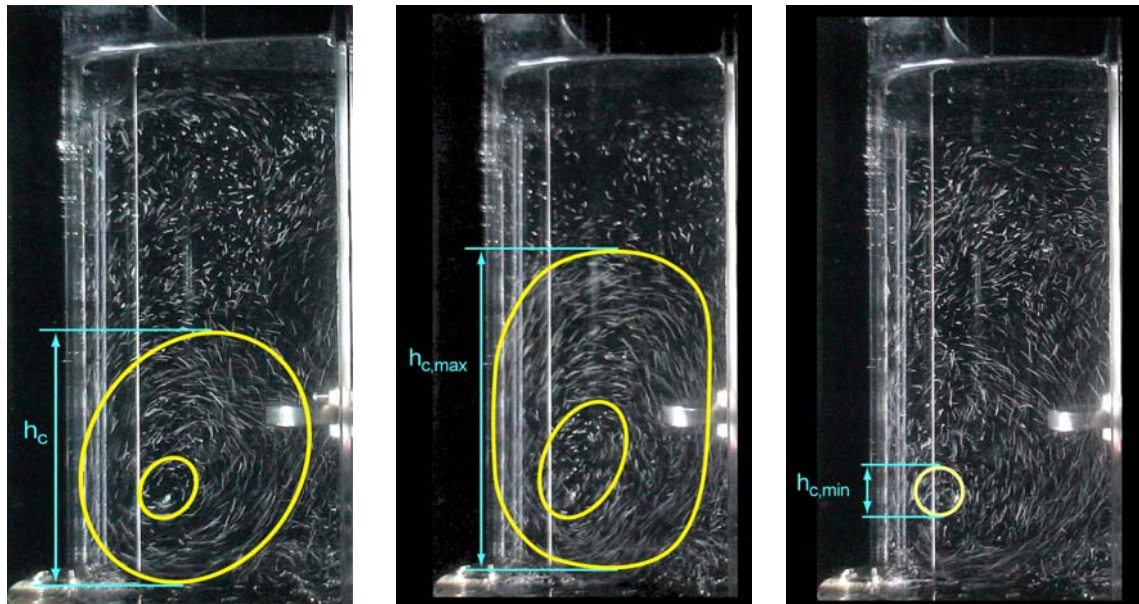


Fig. 5. a) PCL growing

b) PCL at maximum height

c) PCL after its collapse.

The process (oscillation of the PCL) is apparently characterized by a certain periodicity. The function of the incidence of the PCL in time is illustrated in Fig. 6, which shows that the PCL incidence ratio approaches 80% of the considered time.

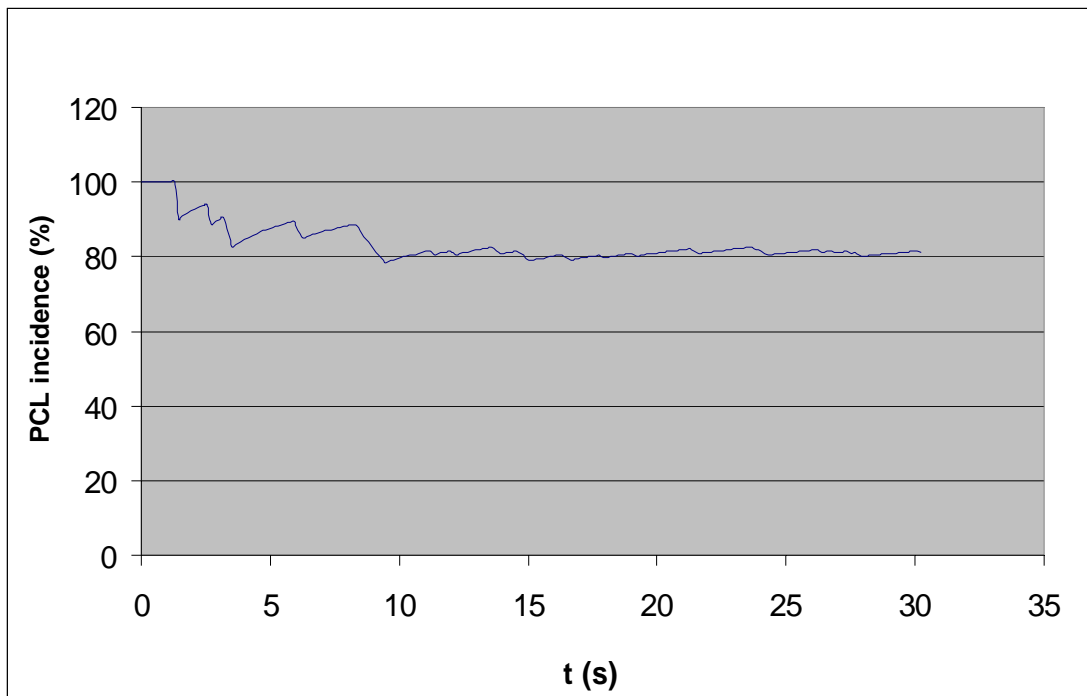


Fig. 6. Dependence of PCL incidence on time for the whole analyzed time.

The graph in Fig. 7 (vertical dimension of the PCL as a function of time) illustrates this process for the whole analysed time of 30.24 s.

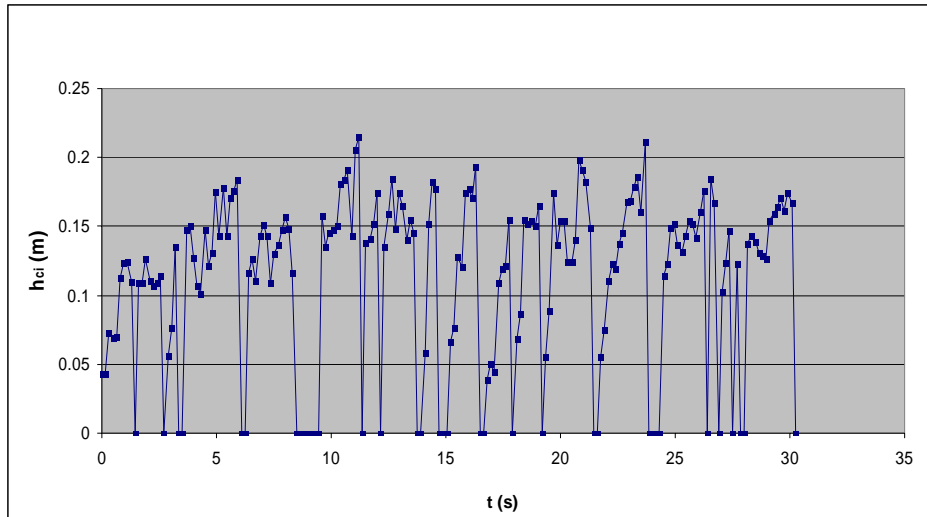


Fig. 7. Dependence of the vertical dimension of PCL h_{ci} on time for the whole analyzed time.

The calculated average time of one cycle (the time between the origin of the PCL and its collapse) is $t_{c,av} = 1.59$ s. This means that the frequency of the PCL oscillations is $f_{osc} = 1/t_{c,av} = 0.63$ Hz and dimensionless frequency $F_{osc} = f_{osc}/n = 0.094$.

This dimensionless frequency is markedly higher than the value detected earlier in the interval 0.02-0.06 [8-10]. This corresponds to our finding that only some of the flow formations generated by one PCL cycle result in macro-flow formation causing a surface level eruption, detected as “macroinstability”.

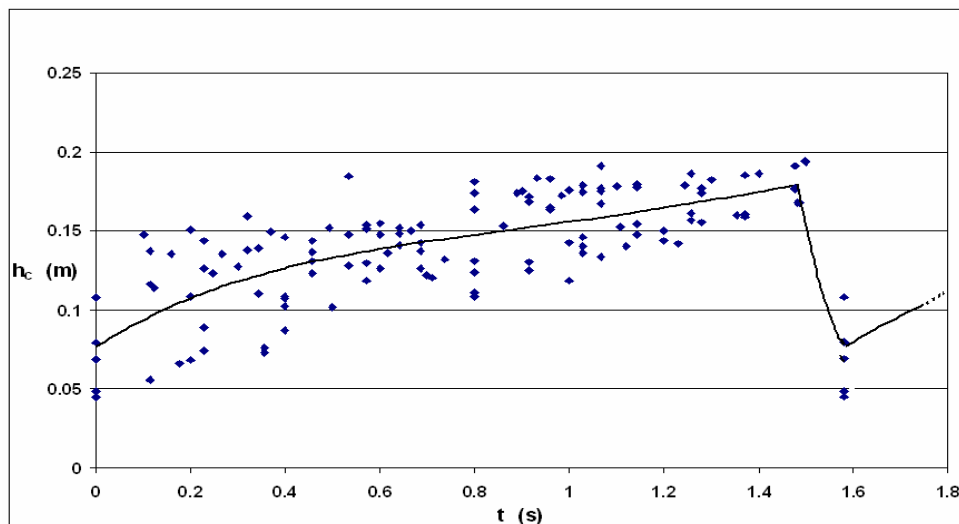


Fig. 8. Time evolution of the height of the PCL (average cycle time $t_{c,av} = 1.59$ s, maximum height $h_{c,max} = 0.181$ m, $h_{c,max}/H = 0.62$) for one cycle of PCL oscillation.

The function $h_c = h_c(t)$ for one cycle is shown in Fig. 8. This function was obtained by regression of the experimental data $h_{ci}(t)$, where the individual cycle intervals were recalculated for an average time cycle $t_{c,av} = 1.59$ s. Fig. 8 shows that the mean maximum height of the PCL $h_{c,max}$ reaches a value of 0.181 m, which is 62% of surface level height H . This agrees with earlier findings [11] that $h_{c,max} \approx 2/3 H$. The function $h_c = h_c(t)$ was used for calculating the PCL rising velocity, see Fig. 9.

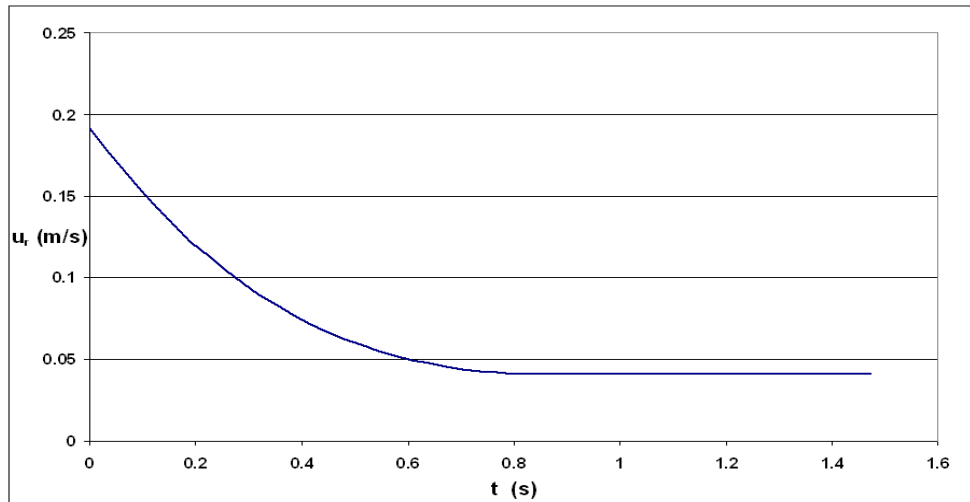


Fig. 9. Dependence of the mean rising velocity u_r of the PCL on time ($u_r = dh/dt = 0.042$ m/s = const., $t > 0.77$ s).

Finally, the average rising time of flow macro formation generated by PCL was calculated from the time function $h_{FMI} = h_{FMI}(t)$ (time between generating and disintegration), and the value obtained was $t_{av, FMI} = 1.0$ s.

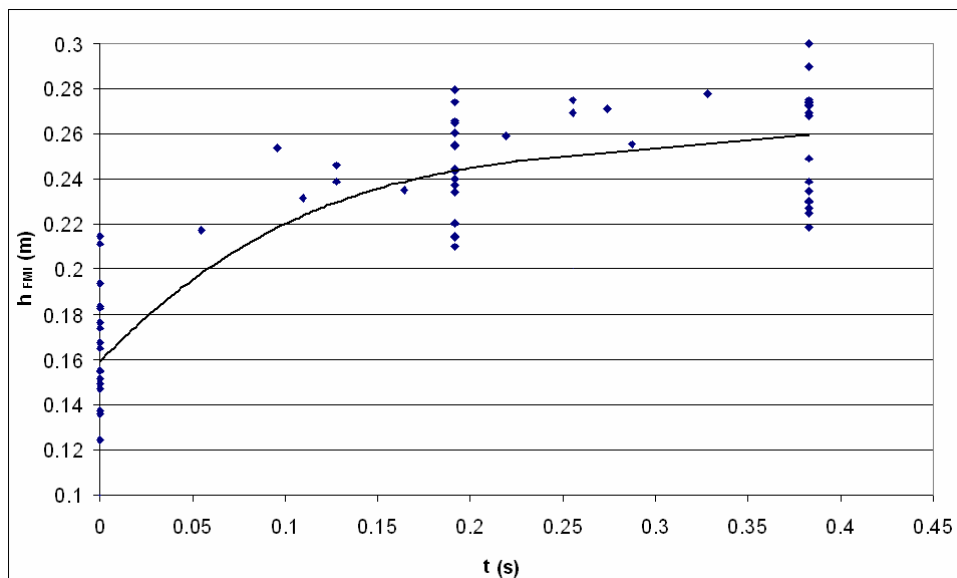


Fig. 10. Dependence of the height of the top of the flow macro formation $h_{FMI,i}$ on the time for one cycle.

The regression curve $h_{\text{FMI},i} = h_{\text{FMI},i}(t)$ corresponding to the experimental data for one cycle (development of one macro-formation, the time recalculated for average rising time $t_{\text{av,FMI}}$) is illustrated in Fig. 10.

To specify the PCL characteristics more deeply, the volume of the PCL (active volume of the primary circulation) was calculated. This was assumed as a toroidal volume around its elliptical projection in the r-z plane of the mixing vessel. The function of the ratio of the PCL volume to vessel volume $V_c/V = (V_c/V)(t)$ for one cycle is illustrated in Fig. 11, where

$$V_c(t) = \frac{\pi^2}{2} \left(\frac{T h_c(t) s_c(t)}{4} - T r_{c,\text{av}}^2(t) \right) \quad (1)$$

is calculated from the corresponding regression curves $h_c = h_c(t)$, $s_c = s_c(t)$ and $r_{c,\text{av}}(t)$. Fig. 11 shows that the mean maximum ratio of the PCL volume to the vessel volume $V_{c,\text{max}}/V$ reaches a value of 0.326.

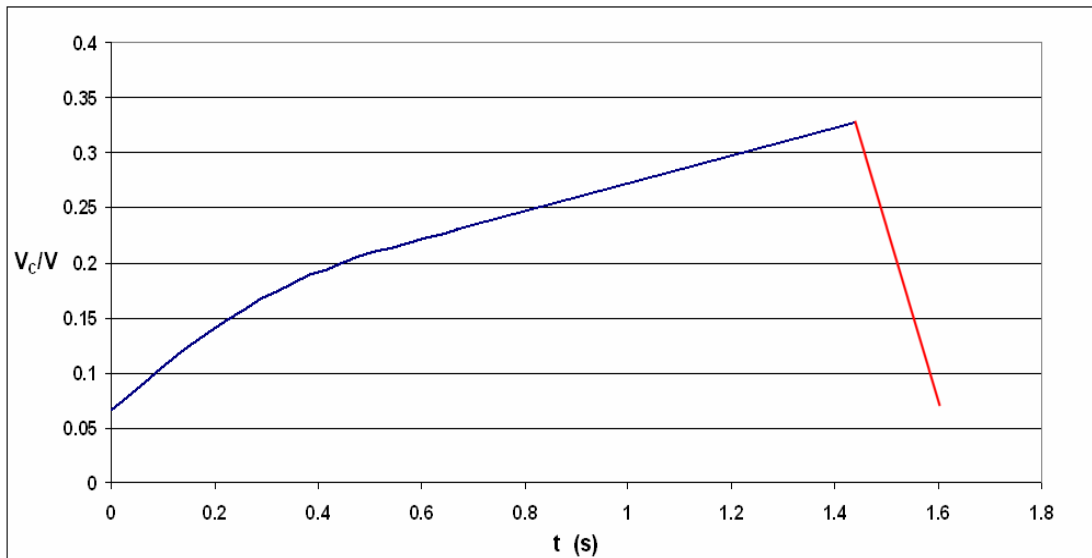


Fig. 11. Dependence of the ratio of the PCL volume to the vessel volume $V_{c,\text{max}}/V$ on time for one cycle of the PCL oscillation.

4. Theoretical calculation of energy balance

An energy balance for the PCL was carried out with a view to explaining the reasons for the flow field behaviour (predominantly PCL oscillations). As mentioned above, there are three different stages in the flow process. The energy balance was carried out for the quasi-steady stage under conditions when the PCL reaches its top position, i.e. $h_c = h_{c,\text{max}}$, see Fig. 12.

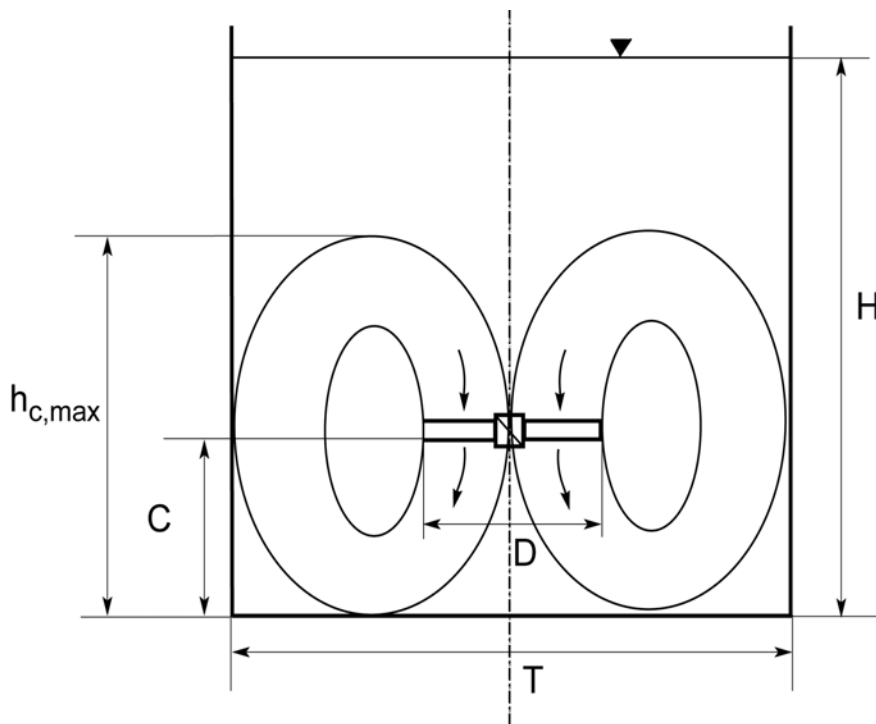


Fig. 12. Schematic view of the PCL under its top position ($h_c = h_{c, \max}$).

This stage directly proceeds (precedes) the collapse and is assumed to have a critical influence on the flow disintegration.

The impeller power input N is dissipated in the PCL by the following components:

I) Mechanical energy losses:

- 1) N_{turn} - lower turn of the primary circulation loop about 180° from downwards to upwards.
- 2) N_{wall} - friction of the primary circulation loop along the vessel wall.

II) Turbulence energy dissipation:

- 1) N_{disch} - dissipation in the impeller discharge stream just below the impeller.
- 2) N_{up} - dissipation in the whole volume of the agitated liquid above the impeller rotor region, i.e. in the space occupied by both the primary and secondary flow.

It is expected that under quasi-steady state conditions (just before the PCL collapses) these components are in balance with the impeller power output. This means that no spare power is available, and that no alternative steady state formation is possible. The individual power components and quantities can be calculated when the validity of the following simplifying assumption for the flow in the PCL is considered:

- 1) The system is axially symmetrical around the axis of symmetry of the vessel and impeller.
- 2) The primary circulation loop can be considered as a closed circuit.
- 3) The cross section of the primary circulation loop (stream tube) is constant.
- 4) The conditions in the primary circulation loop are isobaric.

- 5) The liquid flow regime in the whole agitated system is fully turbulent.
- 6) The character of the turbulence in the space above the impeller rotor region is homogeneous and isotropic.

4.1. Calculation of basic quantities

Impeller power input

$$P = Po \rho n^3 D^5 \quad (2)$$

where the impeller power number $Po = 1.7$ for $Re_M > 10^4$ [12], $n = 6.67 \text{ s}^{-1}$, $D = 0.0967 \text{ m}$, $\rho = 1000 \text{ kg/m}^3$. Then $P = 4.25 \text{ W}$.

The impeller power output can be calculated for known impeller hydraulic efficiency η_h ($\eta_h = 0.48$ for four 45° pitched blade impeller [14]).

$$N = \eta_h P = 2.04 \text{ W} \quad (3)$$

Impeller pumping capacity Q_p can be calculated from the known flow rate number N_{Qp} ($N_{Qp} = 0.94$ for $Re_M > 10^4$ [13]).

$$Q_p = N_{Qp} n D^3 = 5.66 \cdot 10^{-3} \text{ m}^3 \text{ s}^{-1} = 5.66 \text{ ls}^{-1} \quad (4)$$

The mass flow rate is

$$m_p = Q_p \rho = 5.66 \text{ kg s}^{-1} \quad (\rho = 1 \text{ kg l}^{-1}) \quad (5)$$

The axial impeller discharge velocity is equal to the average circulation velocity of the PCL (assuming a constant average circulation velocity in the loop):

$$w_{c,av} = \frac{4Q_p}{\pi D^2} = 0.77 \text{ ms}^{-1} \quad (6)$$

where $\pi D^2/4$ is the cross sectional area of the impeller rotor region, i.e. the cylinder circumscribed by bottom and jacket by the rotary mixer. Then the primary circulation loop is a closed stream tube consisting of the set of stream lines passing through the impeller rotor region.

4.2. Calculation of turbulent dissipation below the impeller rotor region, N_{disch}

The energy dissipation rate per unit mass is [14]

$$\varepsilon = A' \frac{q^{3/2}}{L} \quad (7)$$

where

$$A' = (2/3)^{3/2} \quad (8)$$

and the integral length of turbulence [14] is

$$L=D/10 \quad (9)$$

The kinetic energy of turbulence per unit of mass is

$$q = \frac{1}{2} \left(\overline{w_z'^2} + \overline{w_r'^2} + \overline{w_\theta'^2} \right) \quad (10)$$

According to [14] the average value of q in impeller the discharge stream is $q_0 = 0.226 \text{ m}^2 \text{ s}^{-2}$ for the conditions described in [14]: a four pitched blade impeller with a pitch angle of 45° , $D_0 = 0.12 \text{ m}$, $T_0 = 0.24 \text{ m}$, $n_0 = 6.67 \text{ s}^{-1}$, $P_{O0} = 1.4$, $Re_{M,0} = 44 \cdot 10^4$, $P_0 = 10.3 \text{ W}$, $L_0 = 0.012 \text{ m}$. We have from Eq. (7) $\varepsilon_0 = 6.029 \text{ m}^2 \text{ s}^{-3}$.

The energy dissipation per unit mass ε related to the experimental system used in this study is

$$\varepsilon = \varepsilon_0 \frac{P/m}{P_0/m_0} = \varepsilon_0 \frac{P/V}{P_0/V_0}, \quad (\rho = \rho_0) \quad (11)$$

and after substitution $V = 0.0192 \text{ m}^3$, $P_0 = 10.3 \text{ W}$, $V_0 = 0.0109 \text{ m}^3$ we obtain $\varepsilon = 1.384 \text{ m}^2 \text{ s}^{-3}$.

Using

$$N_{\text{disch}} = \varepsilon \rho V_{\text{disch}} \quad (12)$$

where the dissipation volume below the impeller rotor region $V_{\text{disch}} = 0.000330 \text{ m}^3$ (see Fig. 13). We obtain $N_{\text{disch}} = 0.46 \text{ W}$.

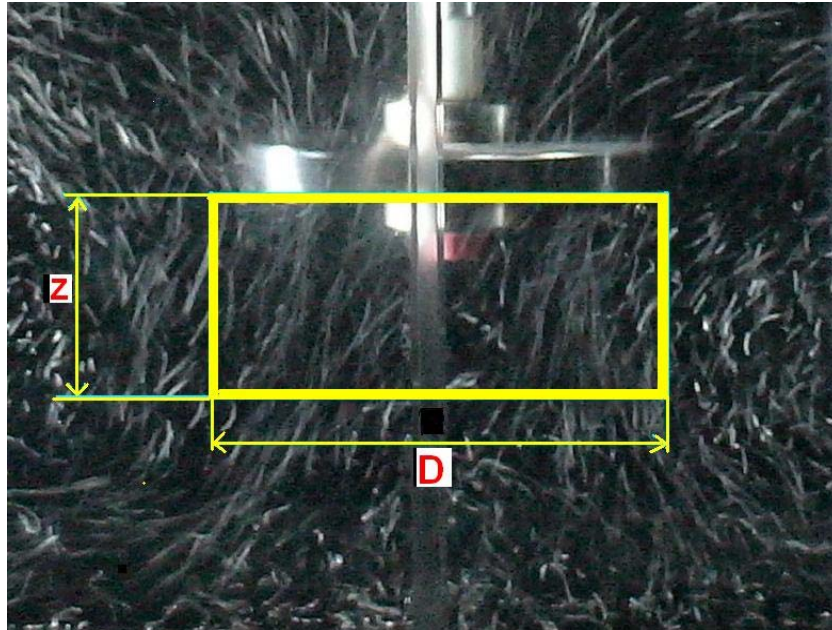


Fig. 13. Dissipation volume below the impeller rotor region V_{disc} before the first turn of the loop ($D = T/3 = 0.0967 \text{ m}$, $z = 0.045 \text{ m}$).

4.3. Calculation of dissipation in the whole volume above the impeller region, N_{up}

According to [15]

$$N_{up} = \eta_{up} P = 0.60 \text{ W} \quad (13)$$

where the portion of the impeller power input dissipated above the impeller rotor region $\eta_{up} = 0.14$ for a six 45° pitched blade impeller ($D/T = C/T = 1/3$, $H = T$) and $Re_M > 10^4$.

When calculating the quantity N_{up} , the validity of introduced assumption No. 6 is considered. Moreover, because of the momentum transfer between the primary flow and the secondary flow out of the PCL the rate of energy dissipation above the impeller rotor region is related to the whole volume, consisting of both the primary and secondary flows.

4.4. Calculation of the dissipation in the lower turns of the PCL, N_{turn}

According to [16]

$$N_{turn} = \sum_j \xi_j \frac{w_{c,av}^2}{2} m_p \quad (14)$$

Substituting the sum of loss coefficients $\sum_j \xi_j = 0.50$ for bend of turn of the PCL $\beta = 180^\circ$ as well as the values of the average circulation velocity of the PCL $w_{c,av}$, and the mass flow rate m_p , we obtain $N_{turn} = 0.84 \text{ W}$.

4.5. Calculation of the dissipation by the wall friction along the PCL, N_{wall}

Using the relation for mechanical energy loss due to the friction along the wall, from [17]

$$N_{wall} = \lambda \frac{l w_{c,av}^2}{d_e^2} m_p \quad (15)$$

where equivalent diameter is defined as

$$d_e = \frac{4S}{O} = \frac{4\pi D^2}{\pi T} = \frac{D^2}{T} \quad (16)$$

and friction factor for a smooth wall

$$\lambda = 0.3164 Re^{-0.25} \quad (17)$$

where

$$Re = \frac{w_{c,av} D \rho}{\eta} \quad (18)$$

Then we can calculate the rate of energy dissipation in the flow along the smooth vessel wall after substitution: $\eta=1$ mPas, length of the PCL along the wall $l = h_{c,max} - h_{turn}$ where $h_{c,max}=0.181$ m, (see Fig. 8), $h_{turn}=0.051$ m, so $l=0.13$ m, and values $d_e = 0.032$ m, $Re = 7.45 \cdot 10^4$ and $\lambda = 0.020$ obtained from Eqs. (16)-(18) to Eq. (15), we get $N_{wall} = 0.14$ W.

4.6. Energy balance in the quasi-steady stage of the PCL

The sum of all dissipated power components considered here is

$$\sum N_i = N_{turn} + N_{wall} + N_{disch} + N_{up} \quad (19)$$

$$\sum N_i = 0.84 + 0.14 + 0.46 + 0.60 = 2.04 \text{ W} \quad (19a)$$

The value in Eq. (19a) is in good agreement with the impeller power output from Eq. (3), $N = 2.04$ W, though the data used for the calculations come from six independent literature sources. This result means that in the quasi-steady phase of the PCL oscillation cycle, all the impeller power output is consumed by dissipation. No power is available, either for increasing the PCL kinetic energy or for any changes in flow formation resulting in a higher energy level. On the other hand, it is well known that vortex disintegration in smaller formations or even a very small vortex separation from a primary flow is a process that consumes energy (according to the law of angular momentum conservation). The experiments proved that vortex separations (small and large) occur in all the stages, thus also in the quasi-steady stage. This seems to provide an explanation for the PCL collapse: in the quasi-steady stage, the energy necessary for vortex separation or for other changes in flow formation cannot be supplied by the impeller, but energy is exhausted from the ambient flow field. And then, even a very small energy deficit can result in a qualitative flow field change appearing as the PCL collapse. It should be noted that the PCL collapse can be followed by a noticeable rise of the surface level, classified as a macroinstability. But not each collapse reaches the level and is observed as a macroinstability. This corresponds to the disagreement between the PCL oscillation frequency determined experimentally in this study and the macroinstability frequency presented in other studies, as mentioned in section 3.

5. Conclusions

- a) The average circulation velocity in the primary circulation loop is more than one order of magnitude higher than the rising velocity of the loop.
- b) The frequency of the primary loop oscillations is about one order of magnitude lower than impeller frequency of revolution.

- c) The top of the disintegration of the primary circulation loop is a birthplace of the flow macroinstabilities in the region of secondary flow.
- d) The primary circulation loop collapses owing to disequilibrium between the impeller power output and the rate of dissipation of the mechanical energy in the loop. A small change (e.g. a small turbulent vortex or a small increase in the primary circulation loop) can have a great effect.

Acknowledgements

The authors of this paper are grateful for financial support from the following Czech Grants Agencies:

1. Czech Grant Agency Grant No. 104/05/2500.
2. Czech Ministry of Education Grant No. 1P05 LA 250.
3. Czech Ministry of Education Grant No. MSM6046137306.

List of symbols

b	width of baffle, m
C	off-bottom clearance, m
d_e	equivalent diameter, m
D	impeller diameter, m
f_{osc}	frequency of PCL oscillations, Hz
F_{osc}	dimensionless frequency of oscillations
h_c	value of height of the PCL obtained by regression, m
h_{ci}	experimental value of height of the PCL, m
$h_{c, max}$	maximal height of the PCL, m
$h_{c, min}$	minimal height of the PCL, m
h_{FMI}	value of height of top of flow macro formation obtained by regression, m
$h_{FMI, i}$	experimental value of the height of the top of flow macro formation, m
h_{turn}	height of turn of the PCL, m
H	height of water level, m
l	length of the PCL adjacent to wall, m
L	integral length scale of turbulence, m
m	mass of liquid in a stirred tank, kg
m_p	mass flow rate, kg s^{-1}
n	impeller speed, s^{-1}
N	impeller power output, W
N_{disch}	turbulent dissipation below the impeller rotor region, W
N_{Qp}	impeller pumping number
N_{turn}	dissipation in lower turns of the PCL, W
N_{up}	dissipation in the whole volume above the impeller rotor region, W
N_{wall}	dissipation by the wall friction of the PCL, W
P	impeller power input, W
Po	impeller power number
q	kinetic energy of turbulence per unit of mass, m^2s^{-2}

Q_p	impeller pumping capacity, $m^3 s^{-1}$
$r_{c,av}$	equivalent mean diameter value of the PCL core, obtained by regression, m
$r_{c,av i}$	experimental value of equivalent mean diameter of the PCL core, m
Re	Reynolds number
Re_M	impeller Reynolds number
S	cross section, m^2
s_c	value of width of the PCL, obtained by regression, m
s_{ci}	experimental value of width of the PCL, m
T	diameter of stirred tank, m
$t_{c,av}$	average time of the PCL cycle, s
$t_{av, FMI}$	average rising time of flow macro formation, s
u_r	rising velocity of the PCL, ms^{-1}
$u_{r,av}$	mean rising velocity of the PCL, ms^{-1}
V	volume of stirred tank, m^3
V_c	calculated volume of the PCL, m^3
$V_{c,max}$	maximum value of calculated volume of the PCL, m^3
V_{disch}	volume of dissipation below the impeller rotor region, m^3
W	width of blade, m
$w_{c,av}$	axial impeller discharge velocity, ms^{-1}
w'_z, w'_r, w'_θ	turbulent velocity fluctuations in individual axis directions, ms^{-1}
z	height of cylindrical volume of dissipation below the impeller rotor region, m
β	bend of turn of the PCL, $^\circ$
ε	energy dissipation rate per unit mass, $m^2 s^{-3}$
η	dynamic viscosity, Pa.s
η_h	impeller hydraulic efficiency
η_{up}	portion of the impeller power input dissipated above the impeller rotor region
λ	friction factor
ρ	density of liquid, $kg m^{-3}$
ζ_j	loss coefficient

References

1. Roussinova, V.T., Kresta, S.M. and Weetman, R., (2003) *Chemical Engineering Science* 58, 2297-2311.
2. Roussinova, V.T., Kresta, S.M. and Weetman, R., (2004) *AIChE Journal* 50-12, 2986-3005.
3. Roussinova, V.T., Grcic, B. and Kresta, S.M., (2000) *Trans I Chem E* 78A, 1040-1052.

4. Fan, J., Rao, Q., Wang, Y. and Fei, W., (2004) *Chemical Engineering Science* 59, 1863-1873.
5. Ducci, A., Yianneskis, M., (2007) *AIChE Journal* 53, 305-315.
6. Fořt, I., Gračková, Z. and Koza, V., (1972) *Collection of Czechoslovak Chemical Communications* 37, 2371-2385.
7. Kresta, S.M., Wood, P.E., (1993) *The Canadian Journal of Chemical Engineering* 71, 52-42.
8. Brůha, O., Fořt, I. and Smolka, P., (1995) *Collection of Czechoslovak Chemical Communications* 60,85-94.
9. Hasal, P., Montes, J-L., Boisson, H.C. and Fořt, I., (2000) *Chemical Engineering Science* 55, 391-401.
10. Paglianti, A., Montante, G. and Magelli, F., (2006) *AIChE Journal* 52, 426-437.
11. Bittorf, K.V., Kresta, S.M., (2000) *Chemical Engineering Science* 55, 1325-1335.
12. Medek, J., (1985) *International Chemical Engineering* 20, 664-672.
13. Brůha, O., Fořt, I., Smolka, P. and Jahoda, M., (1996) *Collection of Czechoslovak Chemical Communications* 61, 856-867.
14. Zhou, G., Kresta, S.M., (1996) *Trans I Chem E* 74 (Part A), 379-389.
15. Jaworski, Z., Fort, I., (1991) *Collection of Czechoslovak Chemical Communications* 56, 1856-1867.
16. Perry, J.H., *Chemical Engineer's Handbook (Fourth Edition)*, McGraw-Hill Book Comp., New York (1963).
17. Brodkey, R.S., *The Phenomenon of Fluid Motions*, Adison-Wesley Publishing Comp., Reading (1967).